JOURNAL OF BACTERIOLOGY, May 1996, p. 2650–2655 Vol. 178, No. 9
0021-9193/96/$04.00+0

Topology of the Phenylalanine-Specific Permease of *Escherichia coli*

JING PI AND A. J. PITTARD*

Department of Microbiology, The University of Melbourne, Parkville, Victoria 3052, Australia

Received 4 December 1995/Accepted 25 February 1996

The PheP protein is a high-affinity phenylalanine-specific permease of the bacterium *Escherichia coli*. A topological model based on sequence analysis of the putative protein in which PheP has 12 transmembrane segments with both N and C termini located in the cytoplasm had been proposed (J. Pi, P. J. Wookey, and A. J. Pittard, J. Bacteriol. 173:3622–3629, 1991). This topological model of PheP has been further examined by generating protein fusions with alkaline phosphatase. Twenty-five sandwich fusion proteins have been constructed by inserting the *'phoA* gene at specific sites within the *pheP* gene. In general, the PhoA activities of the fusions support a PheP topology model consisting of 12 transmembrane segments with the N and C termini in the cytoplasm. However, alterations to the model, affecting spans III and VI, were indicated by this analysis and were supported by additional site-directed mutagenesis of some of the residues involved.

The phenylalanine-specific permease (PheP) is a hydrophobic membrane protein of 458 amino acids that mediates the active transport of phenylalanine into *Escherichia coli* (26). It is highly homologous (60.4% identity) with the general aromatic amino acid permease (AroP) (14) and is a member of a superfamily of permeases, which are involved in the transport of amino acids in bacteria or yeasts (27, 29). In addition, other protein sequences which have greater than 30% identity with PheP have been reported recently; the proteins include YTFD (hypothetical 51.7-kDa transport protein of *E. coli* (5), ANSP (L-asparagine permease of *Salmonella typhimurium*) (16), ROCE and ROCC (amino acid permeases of *Bacillus subtilis*) (11, 12), PROY (proline-specific permease of *S. typhimurium*) (18), LYP1 (lysine-specific permease of *Saccharomyces cerevisiae*) (34), ISP5 (putative amino acid permease of *Schizosaccharomyces pombe*) (32), INA1 (amino acid permease of *Trichoderma harzianum*) (37), VAL1 (valine-tyrosine-tryptophan amino acid permease of *Saccharomyces cerevisiae*) (33), and TAT2 (tryptophan permease of *Saccharomyces cerevisiae*) (33).

Although phenylalanine uptake by PheP is driven by the proton motive force (24), the exact mechanism by which PheP mediates the active transport remains obscure. In this regard, information on the membrane topology of the protein is essential.

The hydropathy plot of Engelman et al. (10) of the deduced amino acid sequence of PheP (26), together with the distribution of positively charged residues (23, 38) and the occurrence of the strong probability of β turns (6), had allowed the prediction of a two-dimensional topological model for PheP, a polytopic integral membrane protein composed of 12 putative transmembrane domains (26) (Fig. 1).

To test this model, we have used a genetic approach involving the construction of PheP-alkaline phosphatase fusions. Alkaline phosphatase requires export to the periplasm to form active enzyme. Thus in general, fusions of the alkaline phosphatase protein, without the leader sequence, to periplasmic domains of a membrane protein exhibit high enzymatic activity, while fusions to cytoplasmic domains exhibit only very low activity (20). We have used the sandwich fusion approach, described by Ehrmann et al. (8), in which the reporter protein (PhoA) is inserted within PheP rather than substituting for different lengths of the carboxyl end of the transport protein. The presence of the entire membrane protein sequence has been shown to give a more accurate picture of membrane protein topology (8). This was first demonstrated in an analysis of the MalF secondary folding pattern (8), the membrane topology of the N-terminal domain of Mdr1 protein (3), and topological analysis of the human β_2-adrenergic receptor (17) and more recently from our laboratory in the analysis of the tryptophan-specific permease (MTR) (31).

Overall, our results support the model of 12 transmembrane spans. However, fusions in periplasmic loops adjacent to spans III and VI, respectively, are inconsistent with the previously proposed model. Consequently, we have modified the model at these two regions to accommodate these new data.

MATERIALS AND METHODS

Bacteria, phages, plasmids, and growth media. Table 1 lists the bacterial strains (all derived from *E. coli* K-12), phages, and plasmids used in this study. The minimal media used were the half-strength medium 56 described by Monod et al. (22) and the 121 salts of Torriani (35), supplemented with 0.2% glucose and required growth factors. Luria agar and Lennox broth were used as complete media. The chromogenic substrate 5-bromo-4-chloro-3-indolylphosphate *p*-toluidine salt (XP; Sigma) was dissolved in dimethylformamide and added to media at 40 μg/ml. Kanamycin was used at a final concentration of 25 μg/ml.

Construction of *pheP'-phoA-'pheP* sandwich gene fusions. Site-directed mutagenesis (36) was used to introduce *Bcl*I restriction sites separately into 25 selected positions within the *pheP* gene, carried on mpMU3137 (Table 1). Mutants were isolated and purified, and the presence of the new *Bcl*I sites was confirmed by sequencing the mutated regions. DNA from mpMU3137 carrying each of the mutated *pheP* genes was transformed into *dam* strain JM110 (40). The replicative form of the M13mp18 derivative DNA was isolated, digested with *Bcl*I, and ligated with the *Bam*HI fragment containing the *'phoA* gene from plasmid pSWFII (8). To prevent transfer of any parental molecules, the ligation mixture was digested again with *Bcl*I before transformation into JM101. The correct orientation of *phoA* insertion was identified by restriction mapping followed by sequencing of both junctions between *pheP* and *'phoA*. The *Bam*HI-*Sal*I fragment containing the gene fusion was then cloned into the corresponding sites on low-copy-number plasmid pLG339 and transformed into strain JP8442 (Table 1). Transformants were selected on minimal medium-kanamycin-XP plates. Isolates containing fusion plasmids with high alkaline phosphatase activities were identified by the blue color, whereas low alkaline phosphatase fusion plasmids (white to pale blue) were screened by restriction mapping to identify those with PhoA insertions.

Alkaline phosphatase activity assays. Overnight cultures of strain JP8442 harboring *pheP'-phoA-'pheP* gene fusion plasmids, grown in half-strength medium 56 supplemented with 0.2% glucose and kanamycin, were diluted 1:20 into

* Corresponding author. Mailing address: Department of Microbiology, The University of Melbourne, Parkville, Victoria 3052, Australia. Phone: (613) 9344 5679. Fax: (613) 9347 1540. Electronic mail address: jingwoo@ariel.ucs.unimelb.edu.au.

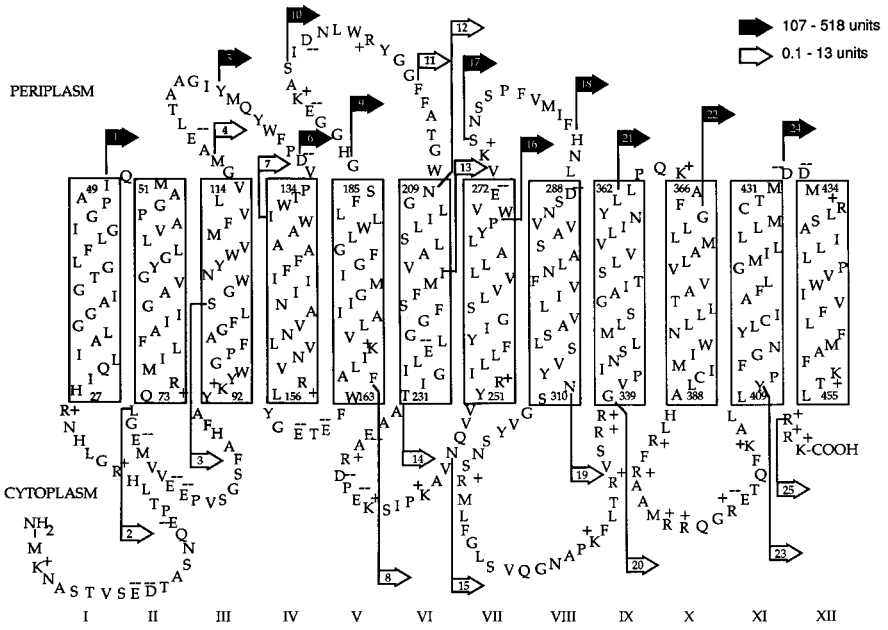

FIG. 1. Proposed membrane topology of the PheP permease (26) showing positions and alkaline phosphatase activities of PheP-PhoA sandwich fusions.

the same medium and grown until the optical density at 600 nm reached 0.4 to 0.55. These cultures were then assayed for alkaline phosphatase activity as described by Manoil (19). The values reported in Table 2 are means of duplicate assays on two to four independent cultures.

[^{14}C]phenylalanine uptake assays. Transport assays were carried out as previously described (39) in the presence of 10 μM L-[^{14}C]phenylalanine (513 mCi/mmol, 50 μCi/ml; NEN/DuPont).

Radiolabelling of fusion proteins. JP8442 cells carrying fusion plasmids were grown under the same conditions as described for the enzyme assay to an optical density at 600 nm of 0.5. Strain W3110 was grown in 121 salts containing 0.2% glucose and 0.1 mM KH_2PO_4, under which conditions expression of the chromosomal *phoA* gene is derepressed (4). For pulse-labelling, 0.5-ml aliquots of cells were incubated for 1 min with 50 μCi of L-[^{35}S]methionine-cysteine (1,175 Ci/mmol, 7.9 mCi/ml; NEN/DuPont), at 37°C before initiation of the immunoprecipitation experiments (see below). For pulse-chase experiments, 2 ml of culture was labelled, and incorporation of [^{35}S]methionine-cysteine was stopped after 1 min by addition of an excess of nonradioactive methionine-cysteine (200 μg/ml). Samples of 0.5 ml were taken after 1, 5, 15, and 30 min for immunoprecipitation.

Immunoprecipitation of fusion proteins. Immunoprecipitations were performed according to the method specific for integral membrane proteins described by Ito and Akiyama (15), using antisera against bacterial alkaline phosphatase (5 Prime→3′ Prime Inc.). Samples were electrophoresed on sodium dodecyl sulfate (SDS)-polyacrylamide gels, and the dry gel was exposed to the X-ray film for at least 24 h. Broad-range protein molecular weight standards (Bio-Rad) were used to estimate the molecular weight of the hybrid protein. The densities of the radioactive bands were measured by scanning the autoradiographs with a Molecular Dynamics scanning densitometer, and these values were used to derive the half-lives of the fusion proteins.

TABLE 1. Strains of *E. coli*, plasmids, and phages used in this study

Strain, plasmid, or phage	Relevant characteristics[a]	Reference
Strains		
JM101	Δ(*lac-pro*) *supE thi* (F′ *tra*Δ*36* *proA*$^+$*B*$^+$ *lacI*^{q} ZΔM15)	21
JP8442	W3110 (Δ*phoA8 tsx*)	30
W3110	Prototroph	1
JP6488	JP777 Δ(*aroP*::Tn*10*) Δ(*pheP367*::Tn*10*)	26
Plasmids		
pSWFII	Ap^r; vector containing *phoA* sandwich fusion cassette	8
pLG339	Km^r Tc^r; low-copy-number cloning vector	28
Phages		
mpMU2148	2.3-kb *Hin*dIII-*Eco*RI *pheP*$^+$ fragment cloned in M13mp18	24
mpMU3137	GTG-to-ATG (at Met-1) mutant of mpMU2148	This study

[a] The genetic nomenclature is that described by Bachmann (2).

RESULTS

Construction of PheP-PhoA sandwich fusions. We have improved the translation efficiency of the *pheP* message by substituting ATG for GTG at the translation initiation codon. This was achieved by site-directed mutagenesis and resulted in increased expression (from plasmid pLG339) of about 3.5-fold (25). We anticipated that this change coupled with the cloning of the various fusions to plasmid pLG339, which has a copy number of six to eight (28), would provide fusions that would give unambiguous distinction between positive and negative values. By introducing *Bcl*I sites within the *pheP* gene (see Materials and Methods), we were then able to insert the *phoA* gene in a *Bam*HI fragment. *Bcl*I sites were positioned so that we could construct at least one fusion in the C-terminal portion of each loop (Fig. 1). Because there were some ambiguities in the hydropathy profile for span III and some mutational studies which suggested a possible different arrangement (27), we constructed two additional fusions in this region at Ser-103 and Met-116. In addition, the results obtained with the initial fusions (fusion 12 [N-209] in particular) were in conflict with the existing model in the region of periplasmic loop III, and three more fusions, 10 (S-193), 11 (F-204), and 13 (I-218), were made to resolve these contradictions.

As described in Materials and Methods, the coding sequence minus the signal sequence of *phoA* was inserted in frame at the various *Bcl*I sites in *pheP*, and the sequences containing the

TABLE 2. Properties of PheP-PhoA sandwich fusion proteins

Fusion	Position of PhoA insertion[a]	Alkaline phosphatase activity (U)	Stability[b] (min)	Transport activity[c]
1	I-49, p	160		0
2	L-74, c	0.6	12	0
3	S-103, III	4	24	0
4	M-116, p	13	9	0
5	Y-125, p	128[d]		0
6	D-132, p	107[d]		0
7	I-137, IV	0.6	3	0
8	F-164, c	10		0
9	G-186, p	172	>30	51
10	S-193, p	463		54
11	F-204, p	12	26	0
12	N-209, p	8	>30	0
13	I-218, VI	13	>30	0
14	T-231, c	7.9		0
15	N-247, c	4		0
16	P-269, VII	466[d]		0
17	S-275, p	518		0
18	H-285, p	385		15
19	N-309, c	6		0
20	N-339, c	6		0
21	L-361, p	331		0
22	G-368, X	138		0
23	Y-410, c	0.1		0
24	D-432, p	341	>30	28
25	R-456, c	11		19

[a] Based on the model shown in Fig. 1. p, periplasm; c, cytoplasm.
[b] Values correspond to the half-life of the fusion protein in minutes derived from pulse-chase experiments.
[c] The specific transport activity for phenylalanine by the wild-type PheP protein is 13 nmol/min/mg (dry weight), and the steady-state level of accumulation is 5.6 nmol/mg (dry weight). Values shown are expressed as percentages of wild-type permease activity as measured by the steady-state level of accumulation.
[d] Colonies from cells expressing the fusion protein are small and dark blue on minimal medium-kanamycin-XP plates and give rise to white colonies after growth in liquid media.

pheP'-phoA-'pheP fusion were cloned into the low-copy-number plasmid pLG339. The various plasmid derivatives were transformed into the Δ*phoA* strain JP8442, and transformants were selected on minimal medium containing kanamycin and the chromogenic substrate XP. On this medium, strains producing high levels of alkaline phosphatase produced blue colonies whereas strains producing low levels of alkaline phosphatase produced white to pale blue colonies. During the isolation of these fusions, we identified three fusions, 5 (Y-125), 6 (D-132), and 16 (P-269), which may, in fact, be toxic to the cell and which appear to be genetically unstable. On the original media they produced small dark blue colonies, but after growth in rich media they gave rise to a significant number of large white colonies.

Alkaline phosphatase activities of PheP-PhoA sandwich fusions. The alkaline phosphatase activity of each of the fusion strains is shown in Table 2, and the position of each fusion in the current topological model is shown in Fig. 1. As can be seen, fusions in each of the putative cytoplasmic loops gave low alkaline phosphatase activity (ranging from 0.1 to 11 U), as would be predicted from the model. The majority of fusions located in the putative periplasmic loops all gave high alkaline phosphatase activities (between 107 and 518 U), as predicted by the model. However, fusion 12 (N-209), located in the periplasmic loop between span V and VI, gave low alkaline phosphatase activity (8 U), unexpected for its presumed periplasmic location. The results of the additional fusions in the earlier part of the loop, fusions 10 (S-193) and 11 (F-204), provided a possible explanation. Whereas fusion 11 (F-204) still gave low enzymatic activity (12 U), fusions 10 (S-193) and 9 (G-186) both gave high values (463 and 172 U, respectively), indicating that the distal part of the loop should be within the membrane.

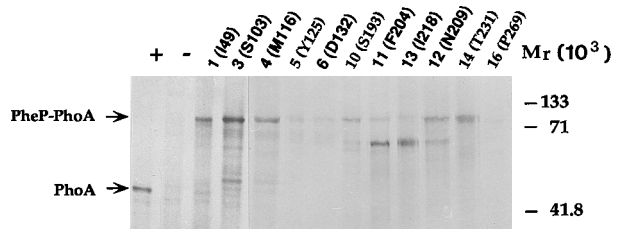

FIG. 2. Immunoprecipitation of [^{35}S]methionine-cysteine-labelled JP8442 cells expressing various PheP-PhoA hybrid proteins. Representative hybrid proteins were pulse-labelled for 1 min before being immunoprecipitated with alkaline phosphatase antibody.

The results for fusion 4 (M-116), located within the putative periplasmic loop between span III and IV, and fusion 7 (I-137), in the beginning of putative span IV, also seem to be at odds with the predictions of the model. The low alkaline phosphatase activities (13 and 0.6 U, respectively) obtained are suggest a location on the cytoplasmic side rather than within or close to the periplasm.

Rate of hybrid protein synthesis. To ensure that the PheP-alkaline phosphatase fusion proteins were being synthesized at approximately the same rate in all of the fusion strains, the rate of synthesis of each was examined by pulse-labelling with [^{35}S]methionine followed by immunoprecipitation of newly synthesized material and analysis on SDS-polyacrylamide gels. All fusions were analyzed by this technique; however, the results of only some representative fusions are shown in Fig. 2.

Some fusions present two discrete bands indicating that the fusion protein has been specifically cleaved. In general, the results confirm that the rates of synthesis of the various fusions appear comparable. Only three strains show a less than normal incorporation of label into alkaline phosphatase; these are fusions 5, 6, and 16, the three which show some genetic instability in rich media. As each of these three has been shown repeatedly to give high alkaline phosphatase activity, the decreased synthesis seen in these gels does not affect the significance of these fusions for confirming the model.

Stability of fusion proteins. To assess the stability of various fusion proteins exhibiting low alkaline phosphatase activity, pulse-chase experiments were carried out as described in Materials and Methods. Results are detailed in Table 2, and some of the gels are shown in Fig. 3.

The examination concentrated on the two regions of the

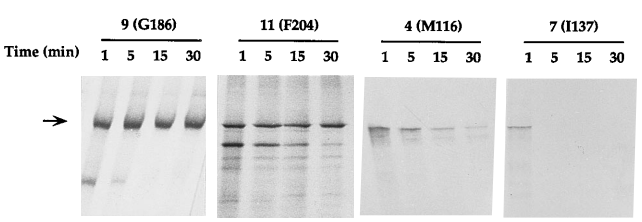

FIG. 3. Stability of PheP-PhoA hybrid proteins. Representative hybrid proteins (fusions 9 [G-186], 11 [F-204], 4 [M-116], and 7 [I-137]) were immunoprecipitated after pulse-labelling for 1 min followed by chase periods of 5, 15, and 30 min. Arrow indicates location of PheP-PhoA.

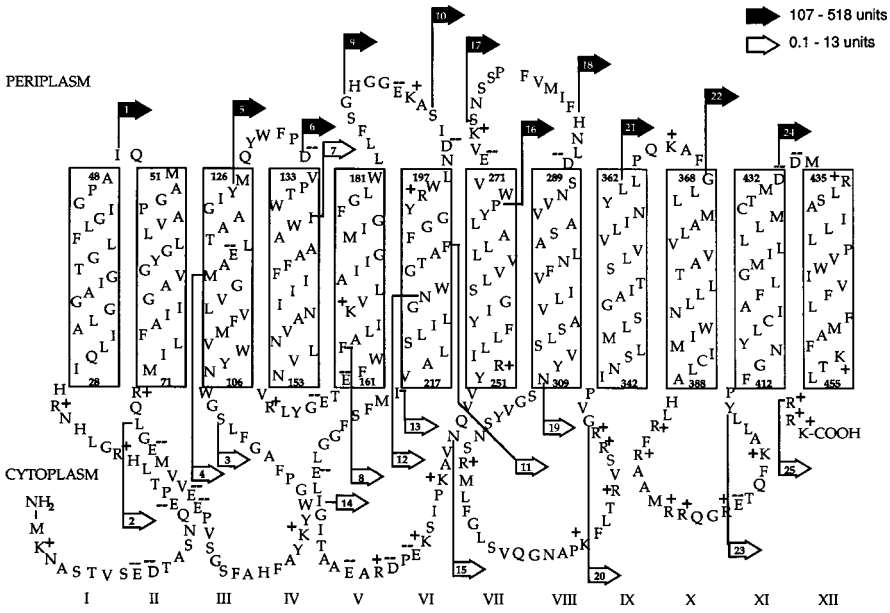

FIG. 4. Modified topological model for the PheP permease based on PheP-alkaline phosphatase fusion analysis and site-directed mutagenesis studies. Twenty-one amino acid residues were used to construct each of the 12 transmembrane segments.

model where alkaline phosphatase activities had been found to be much lower than expected (periplasmic loop III and span VI, and periplasmic loop II and span III). With regard to periplasmic loop III and span VI, fusions 11 (F-204), 12 (N-209), and 13 (I-218) all gave low values of alkaline phosphatase activity. This had been expected only for fusion 13, which had been predicted to be located in span VI. However, as can be seen in Table 2, all three proteins appear to be quite stable, and the low alkaline phosphatase values would not appear to be explained by instability. Fusion 7 (I-137) of span IV is another fusion which gives a very low alkaline phosphatase activity although it appears to be located near the periplasmic margin. As shown in Fig. 3 and Table 2, this fusion protein is highly unstable, with a half-life of 3 min or less, and this instability may well explain the low value.

The second major region of apparent conflict with the model of Fig. 1 lies in the periplasmic loop II and span III. According to Fig. 1, fusion 4 (M-116) should be located in the periplasm, and yet the alkaline phosphatase activity is only 13 U. Whereas the protein is synthesized at a normal rate (Fig. 2), it shows a greater than normal instability, with a half-life of 9 min (Table 2 and Fig. 3), a value similar to that observed for the cytoplasmic fusion 2 (L-74). In contrast, two of the periplasmic fusions tested (fusions 9 and 24) are shown to be much more stable, each with a half-life of longer than 30 min (Table 2 and Fig. 3 show data for fusion 9).

PheP permease activities of fusion proteins. The fusion plasmids obtained were transformed into strain JP6488, and the resulting strains were tested for the ability to transport phenylalanine. The results are shown in Table 2. Apart from fusion 25 (R-456), in which the *'phoA* is inserted in the C-terminal region of *pheP* and is thus predicted to lie in the cytoplasm, all of the other four fusion proteins which transport any phenylalanine at all, fusions 9 (G-186), 10 (S-193), 18 (H-285), and 24 (D-432), are those with *'phoA* gene inserted in the periplasmic region of PheP. The highest transport activities (51 and 54% of wild-type permease activity) were obtained with fusions 9 (G-186) and 10 (S-193), respectively.

The role of Arg-199 in span VI. On the basis of the results obtained with fusions 11 and 12, we have amended the model so that fusion points for these two lie within the membrane (Fig. 4). In the new model, we have positioned Arg-199 at the interface. On the other hand, the fusion result would equally well support a model in which Ile-194 was at the interface and Arg-199 was inserted within the membrane. The high energetic cost of inserting positively charged residues within the membrane, however, ensures that this occurs only when that positively charged amino acid has an essential role to play, either functional or structural, the latter by forming a salt bridge with a membrane-buried negatively charged residue and thereby stabilizing the protein. We tested the importance of Arg-199 by using site-directed mutagenesis to change it to either glycine or serine. In both cases full transport activity was retained, indicating that the positive charge at this position is not essential for biological function. One might compare this finding with the previously reported results for Arg-252, in which case substitution with glycine or serine reduced transport activity to 11 and 31%, respectively (27). Because Arg-199 does not appear to be essential for function, we have retained it at the interface of the lipid bilayer in the new model (Fig. 4).

DISCUSSION

Analysis of the PheP-PhoA fusions presented in this report offer strong general support for the topological model previously proposed for PheP except for two regions: spans III and VI and their associated periplasmic and cytoplasmic loops. In the case of span III, the low alkaline phosphatase activity (13 U) of fusion 4 (M116) would argue against its previous location in the periplasmic loop and favor a location within the membrane. Although this fusion is synthesized at a normal rate, it appears relatively unstable, with a half-life of 9 min, compared with more than 30 min for stable periplasmic fusions. This poses a dilemma which at the moment is not resolved. Is its instability sufficient by itself to explain its low alkaline phosphatase activity, or is it also a consequence of insufficient

transport of alkaline phosphatase into the periplasm? In formulating the previous topological model of Fig. 1, we had been influenced by an ambiguity of the hydropathy profile for span III, which offered two possibilities, and the fact that the alternative as shown in Fig. 1 revealed a sequence of aromatic residues along one face of the helix of this span. Investigation of the importance of these residues by site-directed mutagenesis failed to substantiate a major role for them in transport (27), and reexamination of the hydropathy profile in this region supported an alternative structure as shown in the revised model in Fig. 4. In this model, Met-116 lies in the middle of span III rather than in the periplasm. This particular modification is also supported by topological studies on two other members of the superfamily. In a recent publication describing PhoA fusions with the *E. coli* LysP protein, Ellis et al. (9) suggest a span III which corresponds to the span III of the model in Fig. 4. Parallel studies of alkaline phosphatase sandwich fusions of the very closely related AroP protein also clearly indicate the region homologous to that shown in Fig. 4 as constituting span III (7). Finally, the consequence of the new model is that Glu-118 now lies within the membrane. A negatively charged residue, either glutamate or aspartate, is found at this position in all members of the superfamily (data not shown). Changing this residue to aspartate in PheP reduces transport to 36%, and changing it to glycine, leucine, valine, or asparagine completely abolishes transport activity (27). Within the membrane, this residue and/or Lys-168 of span V, which is conserved in all members of the superfamily, could play an important role in, perhaps, a proton relay system.

In the case of span VI, the results clearly indicate that fusions 11 and 12 are not periplasmic. Even though fusion protein 11 shows some slight instability, this seems insufficient to explain its low activity. As we have already discussed, Arg-199 is nonessential and is probably not inserted in the membrane. This particular residue is not conserved in other members of the superfamily. Although the new model more effectively reflects the alkaline phosphatase activities of the fusion proteins, the low activity of fusion 11 (12 U) compared with the high activity of fusion 16 (466 U) requires further investigation. Unexpectedly, one consequence of the proposed new model in the region of span VI is that Glu-226, which was within the membrane in the old model, is now in the cytoplasm. This glutamate is also absolutely conserved throughout the superfamily, and although it can be substituted by aspartate (129% of wild-type activity), substitution by alanine, glutamine, lysine, arginine, or tryptophan completely abolishes activity (27).

The highest PheP permease activities (about 50% of wild-type permease activity) were obtained with fusions 9 (G-186) and 10 (S-193), both with fusion junctions located in the periplasmic loop III. That these fusion proteins were still able to retain half of the wild-type permease activity indicates that in some cases the PheP permease is able to assume a near-functional, intact tertiary structure, despite the insertion of another large protein. It is of interest that with the exception of the fusion to the last cytoplasmic region at Arg-456, all of the fusions that retain some transport activity involved insertions into periplasmic domains. This may imply that the cytoplasmic loops play a major role in the structure and function of the protein, which is more easily perturbed by insertions of the PhoA sequence. Numerous residues within the cytoplasmic loops such as Arg-26, Glu-226 (25), His-27, Glu-159, Glu-161, and Arg-317 (27) have already been shown to be of major importance for PheP function. Both the new and the old models obey the positive inside rule (38), and both provide a single essential glutamate residue within the membrane, Glu-118 in the new model replacing Glu-226 in the old. Inspection of the new model shows that most spans are flanked at one end or the other by a positively charged residue. Exceptions to this rule are seen in spans III and VIII. These spans, however, are initiated by sequences SGWN and NLDS, respectively, which contain residues with side chain polar groups. One of these sequences, SGWN, has the characteristic features of a so-called capping box (a term that refers to a reciprocal backbone-side chain hydrogen-bonding interaction), frequently observed at the N termini of helices, in which the side chain of the N-cap residue (in this case serine) forms a hydrogen bond with the backbone NH of residue N-3 (in this case asparagine) and the side chain of N-3 forms a hydrogen bond with the NH of the N-cap residue. The capping box appears to act as a helix stop signal (13).

ACKNOWLEDGMENTS

We are grateful to J. Beckwith for providing plasmid pSWFII. We also acknowledge helpful discussions with J. Sarsero. We thank A. Cosgriff, V. Athanasopoulos, J. Yang, and J. Praszkier for the preparation of oligonucleotides, and we thank J.-H. An and Y. Jiang for technical assistance.

This work was supported by Australia Research Council Large Grants Scheme.

REFERENCES

1. **Bachmann, B. J.** 1987. Derivations and genotypes of some mutant derivatives of *Escherichia coli* K-12, p. 1190–1219. *In* F. C. Neidhardt, J. L. Ingrham, K. B. Low, B. Magasanik, M. Schaecter, and H. E. Umbarger (ed.), *Escherichia coli* and *Salmonella typhimurium*: cellular and molecular biology, vol. 2. American Society for Microbiology, Washington, D.C.
2. **Bachmann, B. J.** 1990. Linkage map of *Escherichia coli* K-12. Microbiol. Rev. **54:**130–197.
3. **Bibi, E., and O. Beja.** 1994. Membrane topology of multidrug resistance protein expressed in *Escherichia coli*. N-terminal domain. J. Biol. Chem. **269:**19910–19915.
4. **Brickman, E., and J. Beckwith.** 1975. Analysis of the regulation of *Escherichia coli* alkaline phosphatase synthesis using deletions and ø80 transducing phages. J. Mol. Biol. **96:**307–316.
5. **Burland, V. D., G. Plunkett, and F. R. Blattner.** 1994. Submitted to EMBL/GenBank/DDBJ data banks.
6. **Chou, P. Y., and G. D. Fasman.** 1978. Empirical predictions of protein conformation. Annu. Rev. Biochem. **47:**251–276.
7. **Cosgriff, A.** 1995. Personal communication.
8. **Ehrmann, M., D. Boyd, and J. Beckwith.** 1990. Genetic analysis of membrane protein topology by a sandwich gene fusion approach. Proc. Natl. Acad. Sci. USA **87:**7574–7578.
9. **Ellis, J., A. Carlin, C. Steffes, J. H. Wu, J. Y. Liu, and B. P. Rosen.** 1995. Topological analysis of the lysine-specific permease of *Escherichia coli*. Microbiology **141:**1927–1935.
10. **Engeman, D. M., T. A. Steitz, and A. Goldman.** 1986. Identifying nonpolar transbilayer helices in amino acid sequences of membrane proteins. Annu. Rev. Biophys. Biophys. Chem. **15:**321–353.
11. **Gardan, R., G. Rapoport, M. Debarbouille, Y. Kasahara, and N. Ogasawara.** 1994. Submitted to EMBL/GenBank/DDBJ data banks (no. X81802).
12. **Glaser, P., F. Kunst, M. Arnaud, M.-P. Coudart, W. Gonzales, M.-F. Hullo, M. Ionescu, B. Lubochinsky, L. Marcelino, I. Moszer, E. Presecan, M. Santana, E. Schneider, J. Schweizer, A. Vertes, G. Rapoport, and A. Danchin.** 1993. *Bacillus subtilis* genome project: cloning and sequencing of the 97 kb region from 325° to 333°. Mol. Microbiol. **10:**371–384.
13. **Harper, E. T., and G. D. Rose.** 1993. Helix stop signals in proteins and peptides: the capping box. Biochemistry **32:**7605–7609.
14. **Honore, N., and S. T. Cole.** 1990. Nucleotide sequence of the *aroP* gene encoding the general aromatic amino acid transport protein of *E. coli* K-12: homology with yeast transport proteins. Nucleic Acids Res. **18:**653.
15. **Ito, K., and Y. Akiyama.** 1991. In vivo analysis of integration of membrane proteins in *Escherichia coli*. Mol. Microbiol. **55:**2243–2253.
16. **Jennings, M. P., J. K. Anderson, and I. R. Beacham.** 1995. Cloning and molecular analysis of the *Salmonella enterica ansP* gene, encoding an L-asparagine permease. Microbiology **141:**141–146.
17. **Lacatena, R. M., A. Cellini, F. Scavizzi, and G. P. Tocchini-Valentini.** 1994. Topological analysis of the human β_2-adrenergic receptor expressed in *Escherichia coli*. Proc. Natl. Acad. Sci. USA **91:**10521–10525.
18. **Liao, M. K., and S. Maloy.** 1994. Submitted to EMBL/GenBank/DDBJ data banks (no. X74420).
19. **Manoil, C.** 1992. Analysis of membrane protein topology using alkaline phosphatase and β-galactosidase gene fusions. Methods Cell Biol. **34:**61–75.

20. **Manoil, C., J. J. Mekalanos, and J. Beckwith.** 1990. Alkaline phosphatase fusions: sensors of subcellular location. J. Bacteriol. **172:**515–518.
21. **Messing, J.** 1983. New M13 vectors for cloning. Methods Enzymol. **101:**20–78.
22. **Monod, J., G. Cohen-Bazire, and M. Cohn.** 1951. Sur la biosynthese de la β-galactosidase (lactase) chez *Escherichia coli* La specificite de l'induction. Biochim. Biophys. Acta **7:**585–599.
23. **Nilsson, I., and G. von Heijne.** 1990. Fine-tuning the topology of a polytopic membrane protein: role of positively and negatively charged amino acids. Cell **62:**1135–1141.
24. **Pi, J.** 1991. Ph.D. thesis. University of Melbourne, Melbourne, Victoria, Australia.
25. **Pi, J.** 1993. Unpublished data.
26. **Pi, J., P. J. Wookey, and A. J. Pittard.** 1991. Cloning and sequencing of the *pheP* gene, which encodes the phenylalanine-specific transport system of *Escherichia coli*. J. Bacteriol. **173:**3622–3629.
27. **Pi, J., P. J. Wookey, and A. J. Pittard.** 1993. Site-directed mutagenesis reveals the importance of conserved charged residues for the transport activity of the PheP permease of *Escherichia coli*. J. Bacteriol. **175:**7500–7504.
28. **Pouwels, P. H., B. E. Enger-Valk, and W. J. Brammar.** 1985. Cloning vectors. p. I-A-ii-1. Elsevier Science Publishers, B.V., Amsterdam.
29. **Reizer, J., K. Finley, D. Kakuda, C. L. Macleod, A. Reizer, and J. M. H. Saier.** 1993. Mammalian integral membrane receptors are homologous to facilitators and antiporters of yeast, fungi, and eubacteria. Protein Sci. **2:**20–30.
30. **Sarsero, J. P.** 1994. Ph.D. thesis. University of Melbourne, Melbourne, Victoria, Australia.
31. **Sarsero, J. P., and A. J. Pittard.** 1995. Membrane topology analysis of the *Escherichia coli* K-12 Mtr permease by alkaline phosphatase and β-galactosidase fusions. J. Bacteriol. **177:**297–306.
32. **Sato, S., H. Suzuki, U. Widyastuti, Y. Hotta, and S. Tabata.** 1994. Identification and characterization of genes induced during sexual differentiation in *Schizosaccharomyces pombe*. Curr. Genet. **26:**31–37.
33. **Schmidt, A., M. N. Hall, and A. Koller.** 1994. Two FK506 resistance-conferring genes in *Saccharomyces cerevisiae*, *TAT1* and *TAT2*, encode amino acid permeases mediating tyrosine and tryptophan uptakes. Mol. Cell. Biol. **14:**6597–6606.
34. **Sychrova, H., and M. R. Chevallier.** 1993. Cloning and sequencing of the *Saccharomyces cerevisiae* gene LYP1 coding for a lysine-specific permease. Yeast **9:**771–782.
35. **Torriani, A.** 1966. Alkaline phosphatase from *Escherichia coli*, p. 224–234. *In* G. L. Cantoni, and R. Davies (ed.), Procedures in nucleic acid research. Harper & Row, New York.
36. **Vandeyar, M. A., M. P. Weiner, C. J. Hutton, and C. A. Batt.** 1988. A simple and rapid method for the selection of oligodeoxynucleotide-directed mutants. Gene **65:**129–133.
37. **Vasseur, V. V., M. M. van-Montagu, and G. G. H. Goldman.** 1993. Submitted to EMBL/GenBank/DDBJ data banks (no. Z22594).
38. **von Heijne, G.** 1986. The distribution of positively charged residues in bacterial inner membrane proteins correlates with the trans-membrane topology. EMBO J. **5:**3021–3027.
39. **Wookey, P. J., J. Pittard, S. M. Forrest, and B. E. Davidson.** 1984. Cloning of the *tyrP* gene and further characterization of the Tyrosine-specific transport system in *Escherichia coli* K-12. J. Bacteriol. **160:**169–174.
40. **Yanisch-Perron, C., J. Vieira, and J. Messing.** 1985. Improved M13 phage cloning vectors and host strains: nucleotide sequences of the M13mp18 and pUC19 vectors. Gene **33:**103–119.